2-1-2000

The Lithium-Rotation Correclation in the Pleiades Revisited

Jeremy R. King
Clemson University, jking2@clemson.edu

Anita Krishnamurthi
University of Colorado

Marc H. Pinsonneault
Ohio State University

THE ASTRONOMICAL JOURNAL, 119:859–872, 2000 February

THE LITHIUM-ROTATION CORRELATION IN THE PLEIADES REVISITED

JEREMY R. KING
Department of Physics, University of Nevada, Las Vegas,[1] 4505 South Maryland Parkway, Las Vegas, NV 89154-4002; and Space Telescope Science Institute, Baltimore, MD; jking@physics.unlv.edu

ANITA KRISHNAMURTHI
JILA, University of Colorado and National Institute of Standards and Technology, Campus Box 440, Boulder, CO 80309-0440; anitak@casa.colorado.edu

AND

MARC H. PINSONNEAULT
Department of Astronomy, Ohio State University, 174 West 18th Avenue, Columbus, OH 43210; pinsono@astronomy.ohio-state.edu
Received 1999 July 20; accepted 1999 November 1

ABSTRACT

The dispersion in lithium abundance at fixed effective temperature in young cool stars like the Pleiades has proved a difficult challenge for stellar evolution theory. We propose that Li abundances relative to a mean temperature trend, rather than the absolute abundances, should be used to analyze the spread in abundance. We present evidence that the dispersion in Li equivalent widths at fixed color in cool single Pleiades stars is at least partially caused by stellar atmosphere effects (most likely departures from ionization predictions of model photospheres) rather than being completely explained by genuine abundance differences. We find that effective temperature estimates from different colors yield systematically different values for active stars. There is also a strong correlation between stellar activity and Li excess, but not a one-to-one mapping between unprojected stellar rotation (from photometric periods) and Li excess. Thus, it is unlikely that rotation is the main cause for the dispersion in the Li abundances. Finally, there is a significant correlation between detrended Li excess and potassium excess but not calcium—perhaps supporting incomplete radiative transfer calculations (and overionization effects in particular) as an important source of the Li scatter. Other mechanisms, such as very small metallicity variations and magnetic fields, which influence pre–main-sequence Li burning may also play a role. Finally, we find no statistical evidence for a decrease in dispersion in the coolest Pleiades stars, contrary to some previous work.

Key words: open clusters and associations: individual (Pleiades) — stars: abundances — stars: activity — stars: atmospheres — stars: interiors — stars: late-type — stars: rotation

1. INTRODUCTION

Predictions are made by standard stellar models (e.g., Bahcall & Ulrich 1988) about the surface abundances of elements in stars. However, there are indications that such models are incomplete. A case in point is the surface abundance of the element lithium (Li) in low-mass stars, which is observed to decrease with time.

The solar meteoritic value for the Li abundance is 3.31 ± 0.04 (Anders & Grevesse 1989). A study of Li abundances in young, pre–main-sequence (PMS) T Tauri Stars (TTS) suggests a value of $\log N(\mathrm{Li}) = 3.2 \pm 0.3$ (Magazzu, Rebolo, & Pavlenko 1992), consistent with the meteoritic value. While this is one indicator of the initial Li abundance, TTS abundance determinations are beset by complications due to their youth, such as uncertain $T_{\rm eff}$ estimates and the presence of a circumstellar accretion disk. The study of stars in open clusters of different ages, like α Persei (50 Myr) and the Pleiades (70–100 Myr), shows that there is nearly a uniform Li abundance of 3.2 for high-mass stars ($\sim$7000 K).

It is known that surface Li depletion takes place during the PMS evolution of low-mass stars as a result of Li burning via (p, α) reactions at low temperatures of $T \gtrsim 2.6 \times 10^6$ K. Surface depletion can occur in standard models through convective mixing if the base of the convection zone is hot enough to burn Li (Bodenheimer 1965; Pinsonneault 1997). Because PMS stars have deep convection zones, they burn Li during the PMS. As the depth of the convection zone is a function of mass (increasing with lower mass) Li is depleted on the main sequence only in lower mass stars ($\leq 0.9\ M_\odot$). However, the Pleiades evinces a large dispersion in surface Li abundance at a given color for $T_{\rm eff} \lesssim 5500$ K (e.g., Soderblom et al. 1993b). Standard stellar models are unable to reproduce this dispersion. Furthermore, open cluster observations indicate some depletion is observed on the main sequence as well, which is in conflict with standard models.

Because these models cannot fully explain the observed depletion patterns, additional mixing mechanisms seem necessary. Rotation provides one driving mechanism for such nonconvective mixing, through meridional circulation (Tassoul 1978; Zahn 1992) and instabilities caused by differential rotation (Zahn 1983). Hence, rotation in stars has received much scrutiny as a possible agent of Li depletion and of the observed scatter in open cluster Li abundances at a given mass. Models that include rotational mixing (Pinsonneault, Kawaler, & Demarque 1990) are able to predict the dispersion seen in older systems, but not at young ages like that of the Pleiades (Chaboyer, Demarque, & Pinsonneault 1995). The study of Li abundances is a rich and vast field, and there have been several efforts to study the correlation of surface Li abundances with rotation using stars in open clusters. Here, we concentrate on the connection between surface Li abundance and rotation using data in the young Pleiades cluster.

[1] Current address.

Because the Pleiades Li scatter is such a difficult obstacle in our understanding of early stellar evolution, a historical summary seems in order. Butler et al. (1987) studied a sample of 11 K-stars in the Pleiades and determined that four rapid rotators had higher Li abundances than four slow rotators. They believed this consistent with the evolutionary picture that on arrival on the main sequence, stars had high rotation rates and high Li abundances (i.e., they arrived on the main sequence before there was time for rotational braking or Li depletion). As the star spun down, the Li abundance decreased as well. Hence, they concluded that the faster rotators were younger than the slower, hence less depleted.

A study of the distribution of rotational velocities of low-mass stars in the Pleiades by Stauffer & Hartmann (1987) revealed that there was a wide range of rotation velocities in the Pleiades K and M dwarfs. They showed that the distribution of rotation velocities in the Pleiades could be reproduced quite well invoking angular momentum loss, without having to resort to a large age spread that is also in conflict with the narrow main sequence seen among the low-mass Pleiades stars.

Soderblom et al. (1993b) carried out an extensive study of Li abundances in the Pleiades. They considered several possible explanations for the dispersion in the observed abundances, including observational errors and the effect of starspots. They concluded that the spread in Li abundances seen was real and not an artifact of other physical conditions. They found that the Li abundance was correlated well with both rotation and chromospheric activity, and speculated that rapid rotation was somehow able to preserve Li in stars. While they found some low $v \sin i$ systems with high Li abundances, it was possible that these stars are faster rotators simply seen at low inclination.

Balachandran, Lambert, & Stauffer (1988) studied a sample of stars in the younger α Persei cluster (50 Myr) and concurred with the picture of Li-poor stars as slow rotators. However, a comparison of the Pleiades to α Per by Soderblom et al. (1993b) showed that while most stars had similar abundances, a significant number of stars in α Per had abundances that were less than that in the Pleiades by 1 dex or more. This was difficult to understand until Balachandran et al. (1996) published a corrected list of Li abundances that culled all nonmembers from the sample, bringing consistency to the Pleiades and α Per abundances.

Garcia Lopez et al. (1991a, 1991b) added seven stars to the Butler et al. sample in the range $4500 \gtrsim T_{\rm eff} \gtrsim 5500$ K and asserted a clear connection between Li abundance and $v \sin i$. They also found that the correlation breaks down for temperatures cooler than 4500 K. In a subsequent paper in 1994, they enlarged their sample and further studied the correlation, concluding that their earlier assertion was correct—there were no rapid rotators with low Li abundances and there was a clear relationship between log N(Li) and $v \sin i$. They did note three stars (H II 320, 380 and 1124) having low $v \sin i$ values and Li abundances comparable to those of the rapid rotators as counterexamples, but speculated these objects were rapid rotators seen at low inclination angles. It is to be noted that, when determining mean abundances for their rapid and slow rotator populations, they included the three stars with low $v \sin i$ and high Li abundances in their rapid rotator sample. While this does not change the qualitative result they obtained, it does affect the magnitude of the difference in abundance between the two populations. It also demonstrates that there is a range of abundances for slow rotators.

Jones et al. (1996b) derived Li abundances and rotation velocities for 15 late-K Pleiades dwarfs, and also found that the correlation between Li abundance and rapid rotation breaks down for cooler stars ($T_{\rm eff} \lesssim 4400$ K). Jones et al. (1997) determined rotational velocities and Li abundances in the 250 Myr old cluster M34, intermediate in age between the young Pleiades (70–100 Myr) and the Hyades (500 Myr). They concluded that the Li depletion and rotation velocities were in between the Pleiades and Hyades values, and that the pattern seen in these clusters suggested an evolutionary sequence for angular momentum loss and Li depletion.

One could speculate that some of the Li dispersion in the Pleiades and α Per may be due to non-LTE effects and unknown effects of stellar activity on the Li I line formation (Houdebine & Doyle 1995; Russell 1996; but see Soderblom et al. 1993b). The structural effects of rotation might also be responsible for the Li depletion pattern. Martin & Claret (1996) included this ingredient in their models for masses of 0.7 and 0.8 $M_\odot$ and were able to produce enhanced Li abundances for stars with high initial angular momenta as a result of less effective PMS Li destruction in rapid rotators (i.e., their models imply initially rapid rotators will have high Li abundances relative to the other stars at the same $T_{\rm eff}$ at young ages). Angular momentum loss as well as rotationally induced mixing could affect these models.

The questions we consider here are if there truly is a correlation between Li abundance and rotation rate in the Pleiades, what the nature of the correlation is, and if not, what might explain the abundance scatter. We start with a careful sample selection for our analysis, and examine various possible causes that might contribute to the dispersion (including errors in abundance determination). We then proceed to an analysis of the Li-rotation correlation and explore other possible correlations that might be masquerading as a Li-rotation correlation.

2. PLEIADES LITHIUM ABUNDANCES

2.1. *Sample Selection and Definition*

Lithium abundances were derived from the data sets in the studies of Soderblom et al. (1993a, hereafter S93a) and Jones et al. (1996b). The two studies were merged to form our starting sample with the latter data preferred in cases of overlap. Secondary stellar companions can affect photometric colors from which $T_{\rm eff}$ values are derived, activity levels, measured line strengths, and activity levels deduced spectroscopically. Thus, in order to look at the intrinsic Pleiades Li abundance dispersion unrelated (directly or indirectly) to the presence of a stellar companion, binary systems were excised from our sample. Cluster and interloping field binaries identified by Mermilliod et al. (1992) and Bouvier, Rigaut, & Nadea (1997) were removed from the starting sample. Two spectroscopic binaries not in these lists, but identified as such by S93a, were also removed.

The color-magnitude diagram of this refined sample was then inspected to photometrically identify binaries using the dereddened BVI photometry described by Pinsonneault et al. (1998). We found H II 739 to be an obviously overluminous (or overly red) outlier in the V versus $B-V$, V versus $V-I$, and I versus $V-I$ diagrams, and eliminated it from

the refined sample. Finally, all stars with upper limits on the λ6707 Li I line's equivalent width were eliminated. These upper limits, as censored data, complicate the ensuing statistical analysis. These stars are also the very hottest and very coolest in the sample. Their photometrically inferred $T_{\rm eff}$ values and model atmospheres may be slightly more uncertain than the other objects in the sample. Their elimination simplifies the analysis and reduces possible additional sources of uncertainty.

This final sample of 76 Pleiades stars is listed in the first column of Table 1. The extinction-corrected V magnitude and reddening-corrected $(B-V)$ and $(V-I)$ colors are given in the second, third, and fourth columns. The color-magnitude diagram of these stars evinces a tight main sequence, and is shown in Figure 1 (*open circles*) with a 100 Myr isochrone described in Pinsonneault et al. (1998) and assuming a distance modulus of 5.63 (Pinsonneault et al. 1998). The only possibly discrepant outliers remaining are (1) H II 686, which appears overluminous in the V versus $B-V$ plane, but not the $V-I$ plane, (2) H II 676, which appears underluminous (or too blue) in the $V-I$ plane and perhaps $B-V$ also, and (3) H II 2034, which appears underluminous (or too blue) in the $B-V$ plane, but not in $V-I$. There is no convincing evidence that these slight discrepancies are related to binarity. Rather, they may be due to relatively large photometric errors in one passband or to physical effects (e.g., increased red flux from spots) unrelated to binarity. Stars rejected as binaries are plotted as filled triangles; their general propensity to reside above the main sequence is evident.

2.2. *Stellar $T_{\rm eff}$ and Activity Measures*

S93a and Jones et al. (1996b) provide photometric $T_{\rm eff}$ estimates for all of the stars in Table 1. We reexamine these for comparison and because of concern that chromospheric activity or starspots might affect the colors of young stars.

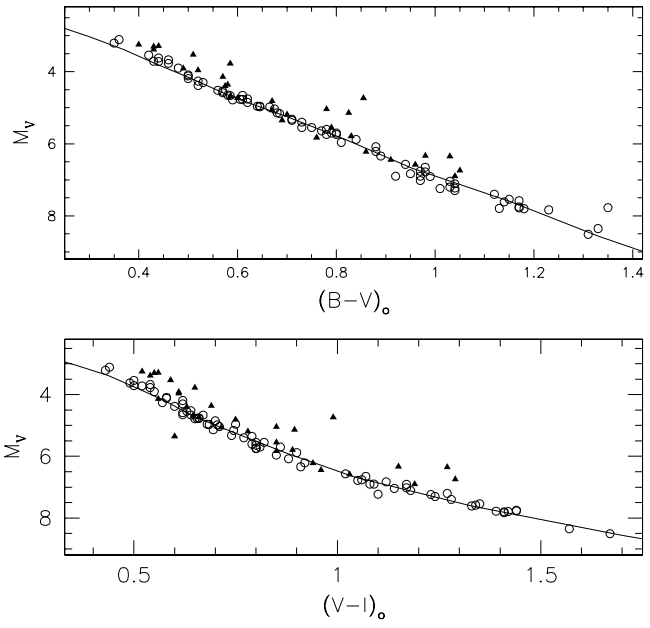

FIG. 1.—Color-magnitude diagrams of our final nonbinary Pleiades Li sample (*open circles*) and stars rejected as binaries (*filled triangles*). The Pleiades data is plotted assuming a distance modulus of 5.63 and with a 100 Myr isochrone from Pinsonneault et al. (1998).

We calculated $T_{\rm eff}$ using our $(B-V)_0$ values and the relation from Soderblom et al. (1993b, equation [3]): $T_{\rm eff} = 1808\,(B-V)_0^2 - 6103(B-V)_0 + 8899$. Temperatures were also derived from our $(V-I)_0$ colors using the relation from Randich et al. (1997): $T_{\rm eff} = 9900 - 8598(V-I)_0 + 4246\,(V-I)_0^2 - 755(V-I)_0^3$. Both of these relations are based on the data from Bessell (1979), and should provide self-consistent temperatures given self-consistent photospheric colors. The fifth, sixth, and ninth columns give the $T_{\rm eff}$ values of S93a, and those derived here from $(B-V)$ and $(V-I)$.

We adopt the Hα- and Ca II infrared triplet-based chromospheric emission measurements from S93a as stellar activity indicators. These are the ratio of the flux (relative to an inactive star of similar color) in the Hα and Ca II lines relative to the total stellar bolometric flux. Given canonical views of a relation between stellar mass and chromospheric emission on the main sequence, it is also of interest to measure the residual Hα and Ca II flux ratios. That is, we wish to detrend the general relation between stellar mass and activity such that activity differences unrelated to large-scale mass differences can be quantified. This was done by fitting the Hα and Ca II flux ratios as a function of $(V-I)$ color temperature with a linear relation,[2] and subtracting this fitted flux ratio (computed at a given $V-I$) from the measured flux ratio of each star. The relation for the fitted Hα flux ratio (used below) was found to be $\log R_{\rm H\alpha,fit} = [-0.00044742 \times T_{\rm eff}(V-I)] - 2.12515$. The relation for the Ca II flux ratio was found to be $\log R_{\rm Ca\ II,fit} = [-0.00021017 \times T_{\rm eff}(V-I)] - 3.50280$.

We find strong evidence that our $T_{\rm eff}$ values (hence, assuming self-consistency of the color-$T_{\rm eff}$ relations, the photometric colors) are affected by activity level. Figure 2 shows the difference between the $(B-V)$- and $(V-I)$-based $T_{\rm eff}$ values versus the Hα flux ratios (*top panel*) and the mass-independent residual Hα flux ratios (*bottom panel*). A relation is seen in both panels, such that the lowest $T_{\rm eff}$ differences are seen predominantly for the lowest flux ratios while the largest $T_{\rm eff}$ differences are seen predominantly for stars having the largest flux ratios. The ordinary linear correlation coefficients are significant above the 99.9% confidence levels for both panels.

The binary stars (*filled triangles*) behave similarly to the single stars in both panels; on average, though, the binaries exhibit larger $T_{\rm eff}$ residuals than the single stars. This systematic offset likely reflects the additional influence of fainter (hence cooler and redder) companions on the photometric colors. If this interpretation is correct, it could suggest that the handful of inactive single stars with significant $T_{\rm eff}$ residuals in the upper left portion of both panels are unrecognized binaries.

Significant differences between the $(B-V)$- and $(V-I)$-based $T_{\rm eff}$ estimates, the slight propensity for $(B-V)$ to yield larger temperatures, and the association of these properties with stellar activity seems to be a common property of young stars noted and discussed by others (e.g., Garcia Lopez et al. 1994; Randich et al. 1997; King 1998; Soderblom et al. 1999). Explanations for these observed properties in young stars are at least twofold: (1) increased B-band flux due to boundary layer emission associated with

[2] Quantitative comparison of the resulting χ^2 values indicated that fits with higher order functions did not yield statistically improved descriptions of the flux ratio-color relations.

TABLE 1

PLEIADES SINGLE-STAR SAMPLE USED

Name (H II)	V	$B-V$	$V-I$	$T_{\rm eff}$[a]	$T_{\rm eff}(B-V)$	EW $(B-V)$	Li $(B-V)$	$T_{\rm eff}(V-I)$	EW $(V-I)$	Li $(V-I)$	σ(EW)	σ(Li) $(B-V)$	σ(Li) $(V-I)$	$\sigma(\Delta{\rm Li})$ $(B-V)$	$\sigma(\Delta{\rm Li})$ $(V-I)$	$P_{\rm rot}$(day)
25	9.35	0.44	0.52	6560	6564	57	2.99	6471	57	2.92	5	0.07	0.07	0.09	0.09	...
34	11.84	0.88	0.92	4900	4928	134	1.94	4996	135	2.03	18	0.14	0.14	0.11	0.10	6.553: (1)
152	10.60	0.645	0.685	5700	5715	150	2.92	5760	150	2.97	12	0.10	0.10	0.08	0.08	4.12 (3)
164	9.40	0.46	0.54	6480	6474	59	2.95	6376	58	2.86	5	0.07	0.08	0.09	0.09	...
193	11.18	0.75	0.80	5320	5339	148	2.51	5352	148	2.52	12	0.11	0.11	0.07	0.07	...
250	10.59	0.645	0.68	5740	5715	141	2.87	5779	141	2.93	12	0.10	0.10	0.08	0.08	...
253	10.59	0.64	0.75	5700	5734	186	3.17	5521	185	2.93	18	0.14	0.14	0.12	0.11	...
263	11.51	0.84	0.90	5060	5048	290	3.10	5051	290	3.10	12	0.13	0.13	0.09	0.09	4.82 (6)
293	10.665	0.675	0.71	5640	5603	125	2.66	5666	125	2.72	12	0.11	0.11	0.08	0.08	4.2: (5)
296	11.33	0.80	0.86	5180	5174	278	3.17	5166	278	3.16	12	0.13	0.13	0.09	0.09	2.53 (3)
314	10.48	0.62	0.70	5840	5810	167	3.12	5703	166	3.01	18	0.13	0.13	0.12	0.11	1.48 (4, 5)
324	12.87	1.01	1.23	4560	4579	210	1.90	4343	210	1.58	15	0.14	0.13	0.09	0.10	0.41 (2)
380	13.21	1.17	1.34	4240	4233	191	1.31	4186	190	1.26	18	0.14	0.13	0.12	0.12	...
405	9.72	0.50	0.58	6320	6300	81	2.99	6194	81	2.90	25	0.22	0.22	0.22	0.22	...
430	11.27	0.77	0.80	5240	5272	151	2.45	5352	151	2.54	18	0.14	0.14	0.10	0.11	...
489	10.295	0.585	0.67	5920	5947	127	3.00	5818	127	2.88	12	0.10	0.10	0.09	0.08	...
514	10.61	0.665	0.705	5660	5640	135	2.76	5684	135	2.80	12	0.11	0.11	0.08	0.08	...
627	9.53	0.48	0.55	6420	6386	82	3.07	6330	82	3.03	5	0.07	0.07	0.08	0.08	...
636	12.28	0.98	1.07	4660	4654	152	1.68	4636	152	1.64	12	0.12	0.12	0.07	0.07	...
676	12.86	1.04	1.10	4400	4507	34	0.61	4575	34	0.70	5	0.13	0.13	0.08	0.08	...
746	11.18	0.73	0.82	5280	5407	98	2.28	5288	98	2.15	18	0.15	0.15	0.13	0.13	...
879	12.67	1.03	1.14	4520	4531	152	1.50	4498	152	1.45	18	0.14	0.14	0.10	0.10	7.39 (1)
882	12.83	1.03	1.27	4500	4531	212	1.84	4282	210	1.50	25	0.18	0.18	0.15	0.16	0.58 (1)
883	12.93	1.04	1.24	4400	4507	46	0.75	4328	45	0.48	18	0.26	0.26	0.24	0.24	7.2 (6)
996	10.29	0.61	0.64	5880	5849	132	2.94	5939	133	3.03	12	0.10	0.10	0.08	0.09	...
1015	10.40	0.61	0.66	5860	5849	145	3.02	5858	145	3.03	12	0.10	0.10	0.08	0.08	...
1032	10.98	0.71	0.79	5400	5477	213	3.06	5385	212	2.95	18	0.15	0.14	0.12	0.12	1.31 (6)
1039	11.97	0.89	0.91	4720	4899	334	3.21	5023	335	3.38	18	0.17	0.16	0.12	0.13	...
1095	11.71	0.88	0.88	5000	4928	137	1.96	5107	139	2.19	12	0.12	0.11	0.07	0.07	...
1110	13.17	1.15	1.35	4240	4272	21	0.06	4173	20	−0.09	18	0.92	1.11	0.92	1.11	...
1122	9.17	0.42	0.50	6640	6655	67	3.12	6568	66	3.07	5	0.05	0.06	0.08	0.09	...
1124	12.20	0.94	1.02	4800	4760	217	2.19	4746	217	2.18	18	0.15	0.15	0.11	0.11	6.05 (1, 5)
1132	9.30	0.46	0.54	6520	6474	46	2.81	6376	45	2.73	5	0.08	0.08	0.09	0.09	...
1139	9.25	0.44	0.49	6580	6564	51	2.93	6618	51	2.96	25	0.32	0.32	0.32	0.33	...
1200	9.82	0.50	0.62	6280	6300	67	2.88	6021	66	2.64	5	0.08	0.08	0.08	0.07	...
1207	10.395	0.605	0.655	5940	5868	141	3.02	5878	141	3.02	12	0.10	0.10	0.08	0.08	...
1215	10.415	0.59	0.65	5900	5928	125	2.97	5898	125	2.95	12	0.10	0.10	0.09	0.09	...
1275	11.33	0.79	0.81	5200	5206	159	2.42	5320	160	2.55	12	0.11	0.11	0.07	0.07	...
1309	9.34	0.43	0.50	6580	6609	42	2.85	6568	42	2.84	25	0.41	0.41	0.42	0.42	...
1332	12.41	0.98	1.05	4640	4654	35	0.82	4679	36	0.87	12	0.22	0.21	0.20	0.19	8.30 (1)
1454	12.74	1.04	1.18	4440	4507	86	1.07	4426	85	0.96	30	0.26	0.26	0.23	0.24	...
1514	10.385	0.62	0.66	5860	5810	161	3.08	5858	161	3.13	18	0.13	0.13	0.12	0.12	...
1531	13.46	1.23	1.41	4220	4128	99	0.67	4102	99	0.65	25	0.20	0.20	0.20	0.20	0.48 (1)
1593	11.03	0.73	0.77	5460	5407	163	2.67	5452	164	2.73	12	0.11	0.11	0.07	0.07	...
1613	9.75	0.50	0.58	6320	6300	103	3.15	6194	103	3.06	5	0.07	0.07	0.08	0.07	...
1653	13.38	1.17	1.44	4220	4233	109	0.86	4069	107	0.66	40	0.29	0.30	0.29	0.30	0.74 (6)

TABLE 1—*Continued*

Name (H II)	V	$B-V$	$V-I$	$T_{\rm eff}^{a}$	$T_{\rm eff}(B-V)$	EW $(B-V)$	Li $(B-V)$	$T_{\rm eff}(V-I)$	EW $(V-I)$	Li $(V-I)$	σ(EW)	σ(Li) $(B-V)$	σ(Li) $(V-I)$	$\sigma(\Delta{\rm Li})$ $(B-V)$	$\sigma(\Delta{\rm Li})$ $(V-I)$	$P_{\rm rot}$(day)
1776.....	10.79	0.685	0.745	5580	5567	140	2.71	5539	140	2.68	12	0.11	0.11	0.07	0.08	...
1794.....	10.28	0.58	0.62	5940	5967	55	2.49	6021	56	2.55	18	0.20	0.20	0.19	0.19	...
1797.....	10.01	0.52	0.60	6240	6214	125	3.22	6107	124	3.13	18	0.14	0.13	0.13	0.13	...
1856.....	9.89	0.52	0.57	6240	6214	85	2.95	6239	85	2.97	5	0.07	0.07	0.07	0.07	...
1883.....	12.54	0.99	1.17	4560	4629	250	2.23	4443	250	1.97	20	0.17	0.17	0.13	0.14	0.2354 (1)
1924.....	10.215	0.57	0.62	6020	6008	141	3.14	6021	141	3.16	18	0.13	0.13	0.12	0.12	...
2016.....	13.43	1.18	1.41	4220	4215	148	1.05	4102	147	0.92	18	0.13	0.12	0.12	0.13	...
2034.....	12.53	0.92	1.09	4760	4815	223	2.31	4595	221	2.00	30	0.21	0.21	0.18	0.18	0.55 (1)
2126.....	11.59	0.81	0.85	5120	5142	151	2.30	5196	151	2.36	12	0.11	0.11	0.07	0.07	...
2244.....	12.46	0.95	1.12	4720	4733	268	2.50	4536	266	2.21	30	0.23	0.23	0.21	0.20	0.57 (2)
2311.....	11.23	0.78	0.79	5240	5239	141	2.36	5385	142	2.53	12	0.11	0.11	0.07	0.07	...
2341.....	10.77	0.68	0.695	5620	5585	140	2.73	5722	141	2.87	12	0.11	0.10	0.08	0.08	8.2 (5)
2366.....	11.37	0.78	0.80	5240	5239	189	2.63	5352	190	2.77	12	0.11	0.12	0.07	0.08	...
2462.....	11.37	0.80	0.80	5200	5174	103	2.05	5352	104	2.26	12	0.12	0.12	0.08	0.08	...
2506.....	10.15	0.56	0.64	6080	6048	108	2.97	5939	107	2.87	18	0.14	0.14	0.13	0.13	...
2588.....	13.24	1.14	1.33	4300	4291	78	0.72	4199	77	0.60	18	0.17	0.17	0.15	0.16	...
2644.....	10.95	0.71	0.74	5520	5477	186	2.89	5557	186	2.98	12	0.11	0.11	0.08	0.08	...
2741.....	12.53	0.97	1.08	4680	4680	91	1.35	4616	90	1.26	30	0.25	0.25	0.23	0.23	5: (4)
2786.....	10.17	0.57	0.63	6040	6008	128	3.06	5980	127	3.03	18	0.13	0.13	0.12	0.12	2.21 (6)
2870.....	12.39	0.97	1.06	4680	4680	69	1.19	4658	68	1.16	12	0.14	0.14	0.10	0.10	...
3019.....	13.41	1.17	1.39	4220	4233	52	0.43	4125	50	0.28	30	0.42	0.43	0.41	0.43	...
3063.....	13.42	1.13	1.42	4300	4311	139	1.13	4091	137	0.85	25	0.17	0.16	0.15	0.17	0.89 (5)
3163.....	12.65	0.97	1.17	4700	4680	222	2.11	4443	220	1.77	30	0.21	0.21	0.18	0.18	0.42 (5)
3179.....	9.93	0.53	0.62	6180	6172	121	3.16	6021	121	3.03	12	0.10	0.10	0.10	0.09	...
3187.....	13.03	1.12	1.28	4300	4332	72	0.73	4268	71	0.64	18	0.18	0.18	0.15	0.16	...

REFERENCES.—(1) Van Leeuwen, Alphenaar, & Meys 1987; (2) Stauffer et al. 1987; (3) Magnitskii 1987; (4) Prosser et al. 1993; (5) Prosser et al. 1995; (6) Krishnamurthi et al. 1998.

[a] From Soderblom et al. 1993.

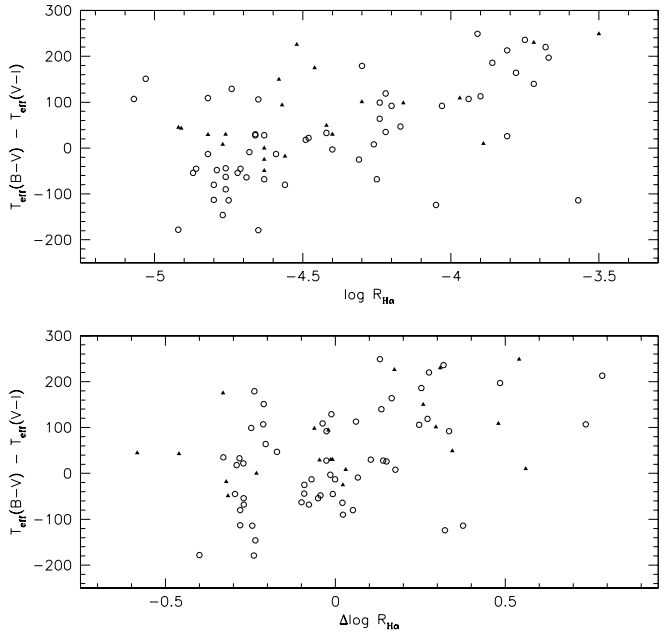

FIG. 2.—Top panel shows the difference between our $(B-V)$- and $(V-I)$-based $T_{\rm eff}$ estimates versus Hα flux ratio (relative to the stellar bolometric flux) from Soderblom et al. (1993a). The bottom panel shows the temperature difference versus the residual Hα flux ratio, which is the flux ratio less a fitted color-dependency.

a circumstellar disk (presumably not applicable for our near-ZAMS Pleiads), and (2) increased I-band flux due to the presence of cool spots. It is straightforward to associate increased prevalence and surface coverage of spots with increasing activity, and Hα emission (used here to quantify activity) has been associated with accretion of circumstellar material in young stars. Given that the Pleiades age ($\sim$100 Myr) is an order of magnitude larger than inferred disk lifetimes for solar-type stars (Skrutskie et al. 1990), spots are the more likely cause of the temperature difference-activity relation in our Pleiades sample. In their recent study of the effects of activity on Pleiades Li abundances, Stuik, Bruls, & Rutten (1997) find that activity—specifically the presence of spots and plages—may significantly alter photospheric colors. Indeed, they suggest that the resulting changes in color may be a more dominant contributor to the Pleiades Li spread than line strength differences. Additionally, they find that such color variations are both surprising and complex. Their empirical solar-based activity models indicated that both spots and plages lead to increased $(B-V)$ colors; in contrast, their "best-effort" theoretical stellar models indicate a decrease in $(B-V)$. Sorting out which (if either) set of models are appropriate for specific Pleiads (in addition to other empirical details such as specific spot/plage coverage and ratio) might be further illuminating. Because the direction of changes in $(V-I)$ also flips in their models, Stuik et al. (1997) note that spot/plage-related changes in color may not be ideally identified in two-color plots (e.g., Soderblom et al. 1993a).

2.3. *Lithium Abundance Determinations and Detrending*

Li abundances for all our Pleiads were determined from the measured λ6707 line strengths and our preferred $T_{\rm eff}$ value. A blending complex lies some 0.4 Å blueward of the Li doublet. In our stars, the typical contribution of these blending features is $\sim$10 mÅ, which is significantly smaller than typical Li line strength of $\sim$100 mÅ. The blending contribution was subtracted[3] following the approach of S93a, who parameterized the contaminating line strength as a function of $(B-V)$ color. Here, we recast this parameterization as a function of $T_{\rm eff}$ so that differences in our $(B-V)$- and $(V-I)$-based temperatures were consistently accounted for in the analysis.

Given the $T_{\rm eff}$ values and the corrected Li line strengths, abundances were calculated using Table 2 from S93a. This was done by fitting a surface map of the equivalent width–temperature abundance grid of S93a using high-order polynomials. The internal interpolation accuracy is generally a few thousandths of a dex[4]. Columns 8 and 11 of Table 1 give the derived Li abundances[5] for our $(B-V)$-based $T_{\rm eff}$, and for our $(V-I)$-based $T_{\rm eff}$.

At the Pleiades age, PMS Li burning has significantly depleted the initial photospheric Li content of many of our stars. Moreover, this PMS depletion is a sensitive function of mass (or $T_{\rm eff}$) with less massive stars having depleted more Li due to deeper convection zones and longer PMS evolutionary timescales. In examining star-to-star Li abundance differences connected with parameters such as rotation or activity, we must remove this general large-scale trend in the abundance-versus-$T_{\rm eff}$ plane.

The procedure is illustrated in Figures 3 and 4, which show the Pleiades Li abundances versus our $(B-V)$- and $(V-I)$-based $T_{\rm eff}$. The familiar and large (3 orders of magnitude) abundance depletion over 2000 K of $T_{\rm eff}$ is seen in Figure 3. The mean trend is shown by the dashed line, which is a fourth-order Legendre polynomial fitted to the single star data after rejecting $\pm 3\,\sigma$ outliers. Fourth-order fits were also conducted for the data based on the S93a temperatures and our $(B-V)$-based values. These fits provide a mean fiducial Li abundance at any given $T_{\rm eff}$ to which observed abundances (calculated assuming the same source of $T_{\rm eff}$) can be compared to infer and measure a relative Li "enhancement" or "depletion" for each star as shown in Figure 4. For $(V-I)$-based temperatures, the approximation to the fit shown in Figure 3 is given by $\log N({\rm Li})_{\rm fit} = -10.8602 + (2.9785 \times 10^{-3} \times T) + (1.1736 \times 10^{-7} \times T^2) - (3.8181 \times 10^{-11} \times T^3)$. For $(B-V)$-based temperatures, the approximation to the fit shown in Figure 3 is given by $\log N({\rm Li})_{\rm fit} = -10.9959 + (2.8360 \times 10^{-3} \times T) + (1.7354 \times 10^{-7} \times T^2) - (4.2744 \times 10^{-11} \times T^3)$.

[3] Deblending corrections were not applied to any stars taken from Jones et al. (1996b) following their claim that instrumental resolution was sufficient to separate the Li line and blending complex. While it is not clear to us that this is true given that some of their objects have appreciable rotation (see their Fig. 1), it does not affect the present results inasmuch as the Jones et al. rapid rotators have Li line strengths significantly larger than those expected of the blending complex.

[4] The two hottest single stars have $T_{\rm eff}$ values significantly outside the curve of growth grids provided by S93a. Extrapolation to these temperatures with high-order polynomials leads to errantly low abundances by a few tenths of a dex. To the extent that we are mainly interested in the cooler Pleiads and that we are interested only in the differential star-to-star Li abundances (i.e., large-scale abundance morphology with $T_{\rm eff}$ is removed later), these known errors are unimportant for the present analysis. In the case of these two stars (H II 133 and 470), we simply caution those who would use our absolute abundances, and also note that the few much smaller extrapolations to lower $T_{\rm eff}$ outside the S93a grid are not believed to be affected by any substantial amount.

[5] By number, relative to hydrogen, on the usual scale with $\log N({\rm H}) = 12$.

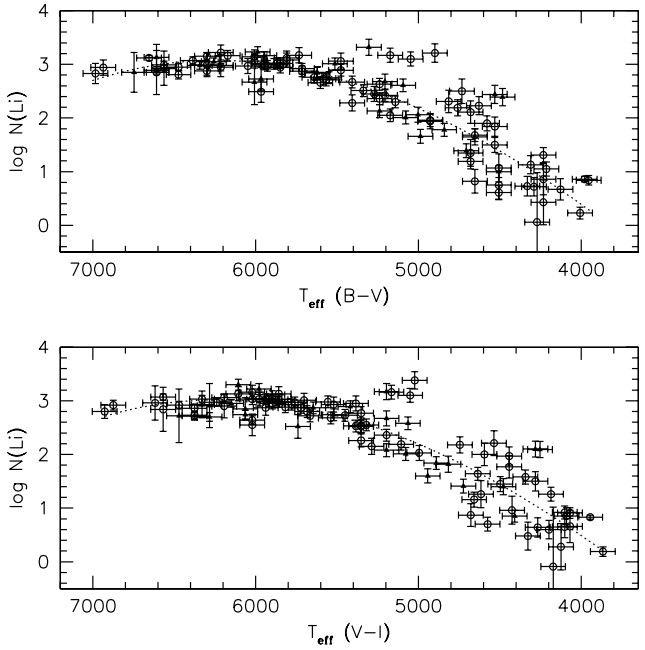

FIG. 3.—Li abundances (with derived errors) vs. $T_{\rm eff}$ from our $(B-V)$ measures (*top*) and $(V-I)$ measures. The well-known declining trend of Li abundance with decreasing $T_{\rm eff}$ is fit with a fourth-order Legendre polynomial (*dashed line*).

2.4. *Errors*

Uncertainties in the Li abundances were estimated from those in $T_{\rm eff}$ and equivalent width. Here, we are interested only in the internal errors that affect the star-to-star Li abundances. A measure of the internal uncertainties in the $T_{\rm eff}$ estimates is provided by the estimates from the $(B-V)$ and $(V-I)$ colors. For the single stars, the difference in the two color-temperatures exhibits a per star standard deviation of 108 K. Assuming equal contributions from both $(B-V)$ and $(V-I)$, this suggests an internal error of ± 76 K in the $T_{\rm eff}$ of any one Pleiad derived from any one color. This uncertainty was translated to a Li abundance error by rederiving abundances with $T_{\rm eff}$ departures of this size. The adoption of identical errors in $(B-V)$ and $(V-I)$-based $T_{\rm eff}$ values is a simplifying assumption (though one likely true within a few tens of K). Inasmuch as our conclusions are the same using either the $(B-V)$ or $(V-I)$ colors, it is not a critical one for this work.

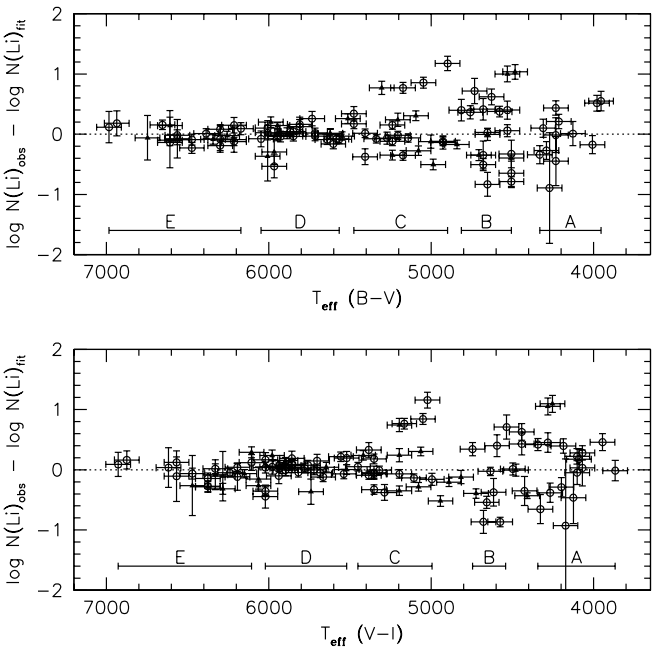

FIG. 4.—Same as Fig. 3, except the differential (detrended) Li abundances and related errors are shown. Temperature bins used in considering the scatter of Li abundances as a function of $T_{\rm eff}$ are labeled in both plots.

The other significant source of uncertainty is in the Li line measurements. For S93a line strengths (the majority of our sample), uncertainties come from their own quality measures: (1) ± 12 mÅ, (2) ± 18 mÅ, (3) ± 25 mÅ, and (4) ± 40 mÅ. Jones et al. (1996b) state that their uncertainties range from 5–20 mÅ and depend largely on projected rotational velocity. Assuming this range and the stars' $v \sin i$ values, we have adopted the reasonable values shown in column 12 of Table 1. Given S93a's note that the equivalent widths of Butler et al. (1987) may have to be regarded with caution, and the typical expected uncertainties from Poisson noise expected from their S/N and resolution, we have assigned an uncertainty of ± 30 mÅ in these line strengths. Based on the S/N, resolution, and $v \sin i$ values of the observations from Boesgaard et al. (1988), we have adopted a conservative uncertainty of ± 5 mÅ for their data. In a similar fashion, we assigned uncertainties of ± 25 mÅ to the equivalent widths from Pilachowski, Booth, & Hobbs 1987). The line-strength uncertainties were translated to Li uncertainties by rederiving abundances with the adopted equivalent width departures.

Final Li abundance uncertainties, shown in Figures 3 and 4, are calculated by summing the two errors in quadrature, and listed in columns 13 and 14 of Table 1. We emphasize that for the purpose of looking at the star-to-star Li abundance differences in cool Pleiads, the effects of $T_{\rm eff}$ errors are minimized. This is because the movement of a star in the $T_{\rm eff}$-Li plane due to $T_{\rm eff}$ errors is very nearly along the cool star depletion trend for $T_{\rm eff} \lesssim 5800$ K. To take into account this correlation in looking at the *differential* Li abundances (i.e., the actual values vs. an expected value from a fitted trend to the data), the abundance errors due to departures in $T_{\rm eff}$ were combined with the slope of the fitted Li versus $T_{\rm eff}$ trend at the $T_{\rm eff}$ of each star. The total uncertainties in the differential Li abundances are given in the final two columns of Table 1.

2.4.1. *Li Abundance Scatter*

Large scatter in the star-to-star Li abundances is apparent in Figures 3 and 4. Comparison of the observed scatter with that expected from the estimated uncertainties indicates that the spread is statistically significant. The presence of real global scatter was considered by comparing the variance of the differential Li abundances with that based on the uncertainties given in Table 1. The sizable reduced χ^2 statistic ($\chi^2_\nu = 12.78$, $\nu = 72$) indicates probabilities of the observed variance [$s(\mathrm{Li})^2 \sim 0.13$ dex^2] occurring by chance are infinitesimal.

Additional analysis was carried out by binning in $T_{\rm eff}$. For both the $(B-V)$ and $(V-I)$ based results, we broke the data up into five $T_{\rm eff}$ ranges following natural breaks in the estimated $T_{\rm eff}$ values, which yielded comparable sample sizes (10–15 stars) in each bin. The results for both the $(B-V)$ and $(V-I)$ data are similar.

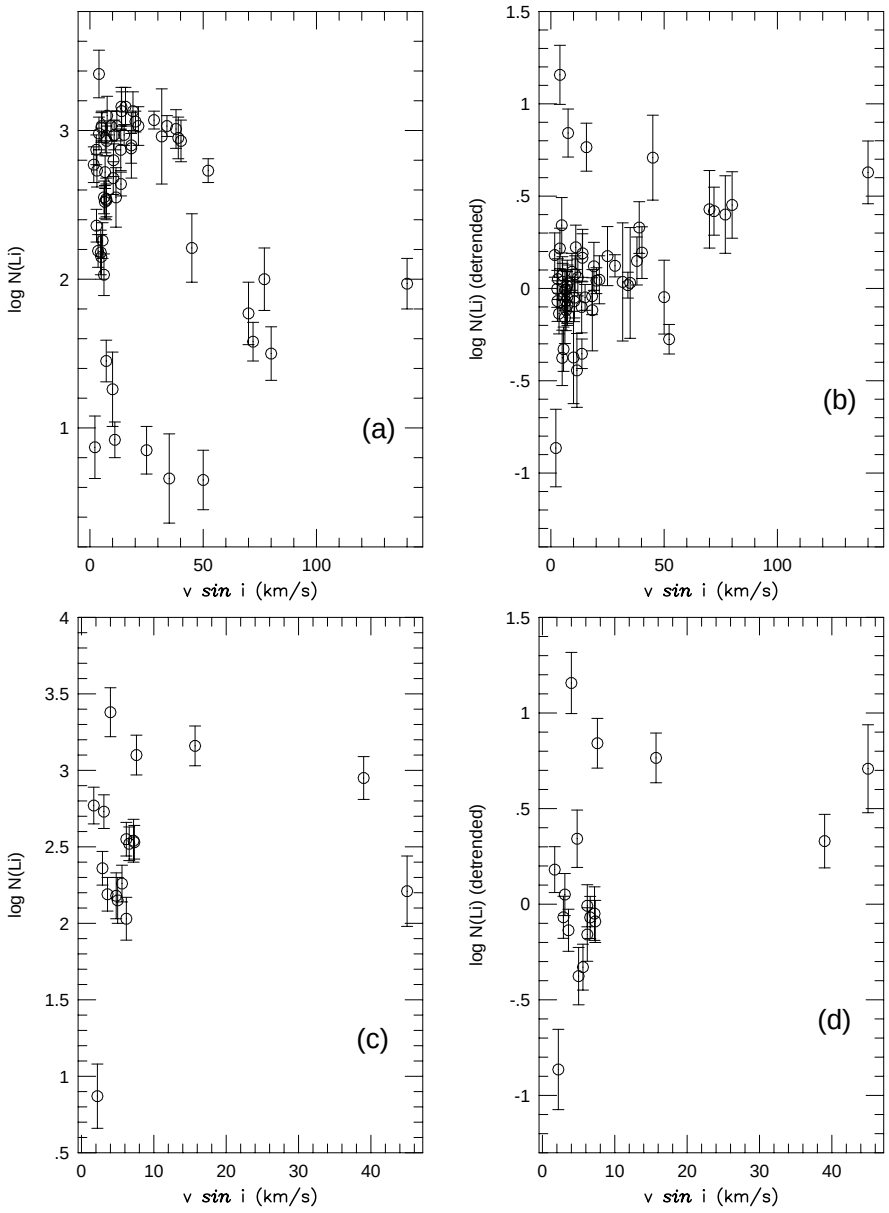

FIG. 5.—Projected rotational velocity v sin i vs. $(V-I)$-based Li results for (*a*) all $T_{\rm eff}$ and absolute Li abundance (*b*) all $T_{\rm eff}$ and differential detrended Li abundance (*c*) $T_{\rm eff}$ = 4500–5500 K and absolute Li abundance (*d*) $T_{\rm eff}$ = 4500–5500 K and differential Li abundance.

We find that stars in the hottest bin (bin E: 6172–6984 K and 6107–6928 K for $B-V$ and $V-I$) exhibit a variance that is larger than the expected value at only the 94% confidence level. The stars in the adjacent cooler bin (bin D: 5567–6048 K and 5521–6021 K for $B-V$ and $V-I$) exhibit a variance in the Li abundances significantly larger than expected from the uncertainties at the $\gtrsim$99.93% confidence level. The differential Li abundances in the remaining three cooler bins (bin C: 4899–5477 K and 4996–5452 K; bin B: 4507–4815 K and 4542–4746 K; bin A: 3955–4332 K and 3867–4343 K) all show observed variances significant at considerably higher confidence levels.

An important claim by Jones et al. (1996b) in their study of Pleiades Li abundances is a progressive decline in the dispersion of the Li abundances as one proceeds from the late-G dwarfs, to the early-to-mid K dwarfs, and finally to the later K dwarfs. We find, however, that quantitative analysis fails to provide firm support for such a conclusion. F-tests of the observed variances indicate that differences of the differential Li abundance dispersions in our cooler three bins are statistically indistinguishable. The differences between the bin B and bin A stars' variances are significant at only the 71.5% and 78.0% confidence levels for the $B-V$ and $V-I$ data sets. Differences between the bin C and bin B stars' variances are different at only the 72.7% and 75.0% confidence levels. It should be noted that these comparisons ignore the observed Li upper limits prevalent for the coolest (bin A) Pleiads. The stars with upper limits lie at the lower edge of the observed Li abundances (Fig. 4 of Jones et al.). Ignoring this censored data may lead to an underestimate of the true dispersion for the coolest Pleiads– making our conclusion of no significant difference in the magnitude of star-to-star abundance scatter for the late-G to late-K Pleiads a conservative one. Larger samples and improved

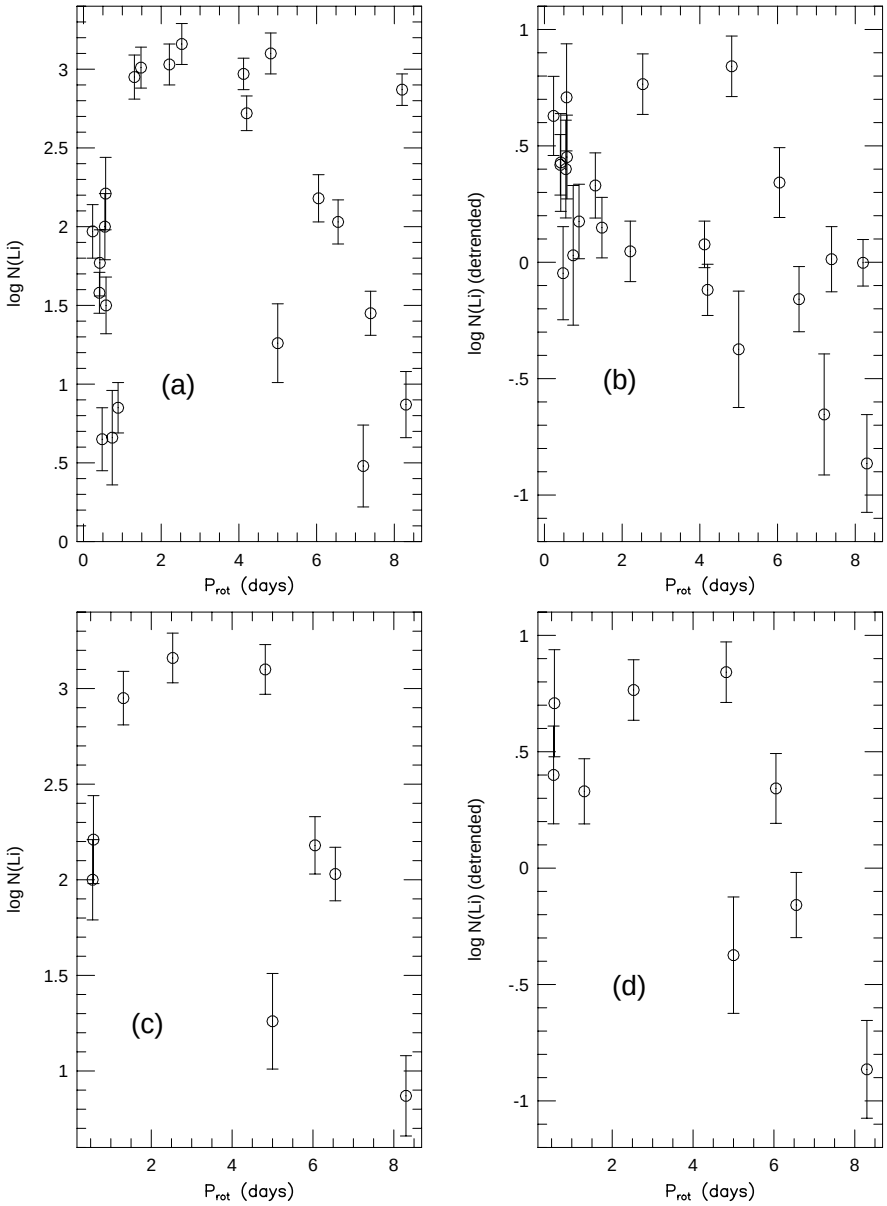

FIG. 6.—Same as Fig. 5, except rotational period, P_{rot}, in days is plotted instead of v sin i

upper limits (or detections) would clarify this important issue.

3. NATURE OF THE Li-ROTATION CORRELATION

3.1. *Projected Rotational Velocity*

Extant studies of Li-rotation correlations have employed v sin i measurements, which yield only a lower limit to the rotational velocity due to the unknown angle of inclination, i. In Figure 5, our $V-I$-based absolute and differential Li abundances are plotted against the projected velocity measurement v sin i. The top two panels (*a* and *b*) show the data for all $T_{\rm eff}$. The bottom two panels (*c* and *d*) show data with $4500 \leq T_{\rm eff} \leq 5500$ K, which is the temperature range in which a clear connection between Li abundance and v sin i was asserted by Garcia Lopez et al. (1994). It is seen that while there is a range of abundances at the lower values of the rotation velocity, the rapid rotators (v sin $i \gtrsim 30$ km s^{-1}) do show a tendency to have higher Li abundances in the intermediate $T_{\rm eff}$ range (*panel d*).

3.2. *Rotational Period*

The Pleiades now has many members with photometrically determined rotation periods (Krishnamurthi et al. 1998), which are free of the ambiguity associated with inclination angle. Hence, it is now possible to consider the true nature of the correlation between rotation and Li abundance. For example, we find a slowly rotating star (H II 263, $P = 4.8$ d) that has a high Li abundance. Furthermore, two of the three stars (H II 320 and 1124) in the Garcia Lopez et al. (1994) study with low v sin i and high Li abundances also have measured rotation periods of 4.58 and 6.05 days respectively. Thus, *there are several cases in which high Li abundance in stars with low* v sin i *is not due to inclination angle effects*—Li overabundances are not solely restricted to rapid rotators. This is apparent in Figure 6, where the surface Li abundance is plotted against rotation period, $P_{\rm rot}$, instead of v sin i. In particular, we draw attention to the large range in abundances seen at longer rotation periods (>4.0 days; *panels b* and *d*). Thus there exist at least

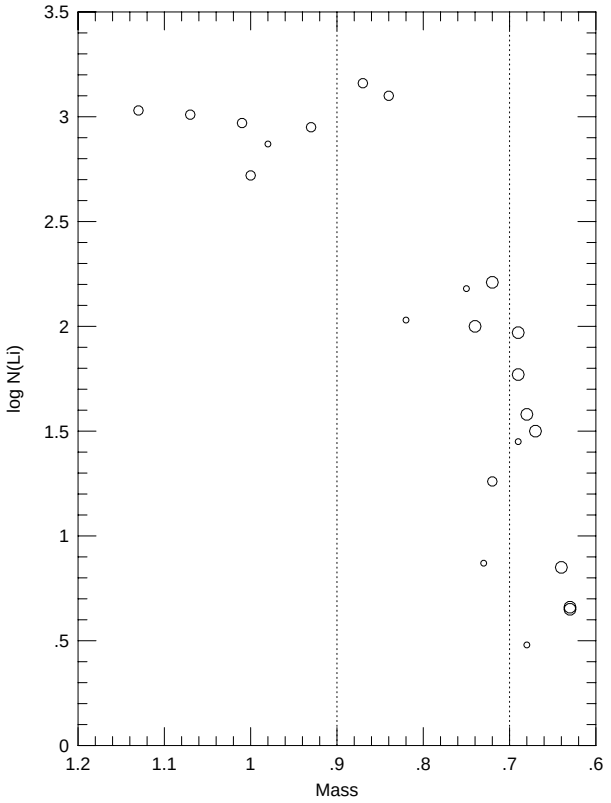

FIG. 7.—Our $(V-I)$-based Li abundances versus stellar mass. The symbol size corresponds to rotational period. The largest circles represent stars with $P_{rot} < 1$ day, the medium sized circles represent those with P_{rot} between 1 and 5 days, while the smaller circles indicate stars with P_{rot} between 5 and 10 days. The dashed lines denote the mass range $M = 0.7$–$0.9\ M_{\odot}$.

a few Pleiads that are true slow rotators, but have high Li abundances.

We next examined the proposal by Garcia Lopez et al. (1994) that there is a very clear relationship between rotation and log N(Li) for stars with $M \sim 0.7$–$0.9\ M_{\odot}$. Figure 7 shows the $V-I$-based Li abundances versus mass for Pleiads with photometrically measured rotation rates. The symbol size is proportional to the rotation period. When rotational periods are considered rather than $v \sin i$ measurements, a true range of Li abundances with rotation is seen in the mass range 0.7–0.9 $M_{\odot}$—there are genuine slow rotators with abundances similar to the fast rotators. Thus, there appears to be a range of rotation at all abundances. Hence, P_{rot} is essential to study the true correlation.

3.3. *Structural Effects of Rotation*

Rapid rotation affects the structure of a star and hence the derived mass at a given T_{eff} (Endal & Sofia 1979). The structural effects of rotation would alter a star's color such that rapidly rotating objects would be redder, hence perceived as cooler, and thus be assigned a lower mass. We therefore examined the abundances as a function of mass rather than effective temperature.

To investigate this issue, it was necessary to construct stellar models for different disk lifetimes (Krishnamurthi et al. 1997). We ran models for $\omega_{crit} = 5 \times \omega_{\odot}$ and $10 \times \omega_{\odot}$ to represent fast rotators and the slow rotators. The rotation-corrected masses were derived by interpolation in the models across effective temperature and rotation velocity for different disk lifetimes. We found that the percent change in mass is small (5%) even for the most rapidly rotating star in the Pleiades (H II 1883, $v \sin i = 140$ km s^{-1}). The change is between 1% and 2% for stars with $v \sin i$ in the 50–100 km s^{-1}, and less than 1% for $v \sin i \leq 50$ km s^{-1}. These small alterations fail to eliminate the Li dispersion, which sets in at $M < 0.9\ M_{\odot}$ in the Li-mass plane. Thus, the structural effects of rotation on the derived mass-temperature relation are not large enough to account for the Pleiades Li abundance dispersion.

These results differ with those of Martin & Claret (1996), who also explored the structural effects of rotation and found enhanced Li abundances for stars with high initial angular momentum. This is not seen in our models, which predict small rotational structure effects on the Pleiades Li abundances, similar to the models of Pinsonneault et al. (1990). Mendes, D'Antona, & Mazzitelli (1999) have noted the conflict between the results of Martin & Claret (1996) and Pinsonneault et al. (1990), and considered the hydrostatic effects of rotation on stellar structure and Li depletion using their own stellar models. Their results are in agreement with Pinsonneault et al. (1990), and they too find that hydrostatic effects are too small to explain the observed Li abundance spread in the Pleiades.

4. Li AND STELLAR ACTIVITY

4.1. *Li and Chromospheric Emission*

Since the large Pleiades Li spread is in such a young cluster, one may wonder if its long-sought explanation is related to stellar activity. Additionally, since rotation and activity are well-correlated, a Li-activity relation may be masquerading as a Li-rotation relation instead. Here, we discuss if magnetic activity indicators such as chromospheric emission (CE) are correlated with the Li abundance. Several studies have pointed out that activity is correlated with the Li abundance (e.g., Soderblom et al. 1993b, Jones et al. 1996a). There have also been some studies speculating that CE affects the *apparent* abundance of Li (e.g., Houdebine & Doyle 1995) and hence may be at least partly responsible for the dispersion.

Figure 8 contains our results, and shows the $V-I$-based differential Li abundances versus the Ca II infrared triplet fluxes (*top panel*) and residual fluxes (*bottom panel*). A relation is seen in both panels, such that the lowest log N(Li) differences are seen predominantly for the lowest flux ratios while the largest log N(Li) differences are seen predominantly for stars having the largest flux ratios. The ordinary correlation coefficients are significant at the 99.7% and $\geq$99.9% confidence levels for the chromospheric Ca fluxes and residual fluxes, suggesting a significant relation between chromospheric activity differences and Li abundance differences (though not necessarily causal).

4.2. *Spreads in Other Elements*

Important clues to the cause of the Pleiades Li abundance scatter can be found from examination of other elements not destroyed in stellar interiors like ^{7}Li. Variations in such abundances may signal effects other than differential Li processing, and perhaps point to an illusory difference caused by inadequate treatment of line formation.

4.2.1. *Potassium*

One of the most useful features for this purpose is the λ7699 K I line. The usefulness of this feature is twofold.

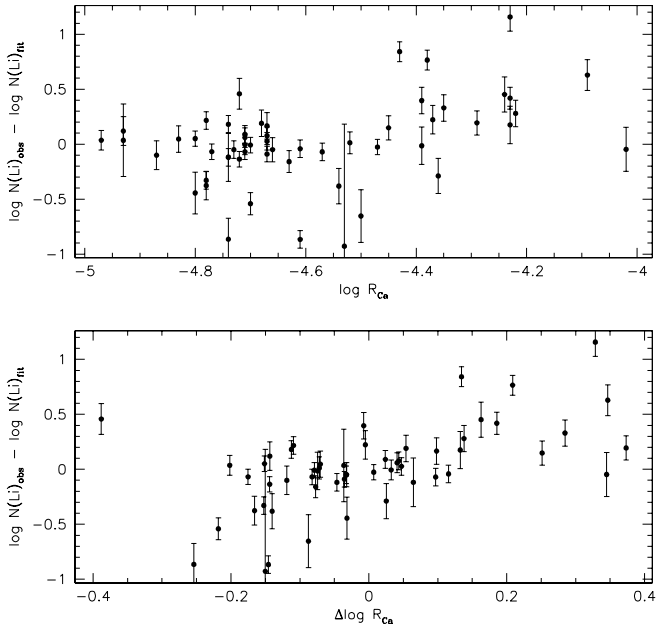

FIG. 8.—Our $(V-I)$-based differential Li abundances are plotted versus the Ca II infrared triplet flux ratio (*top panel*) and residual flux ratio (*bottom*), which is the flux ratio less a fitted color-dependency.

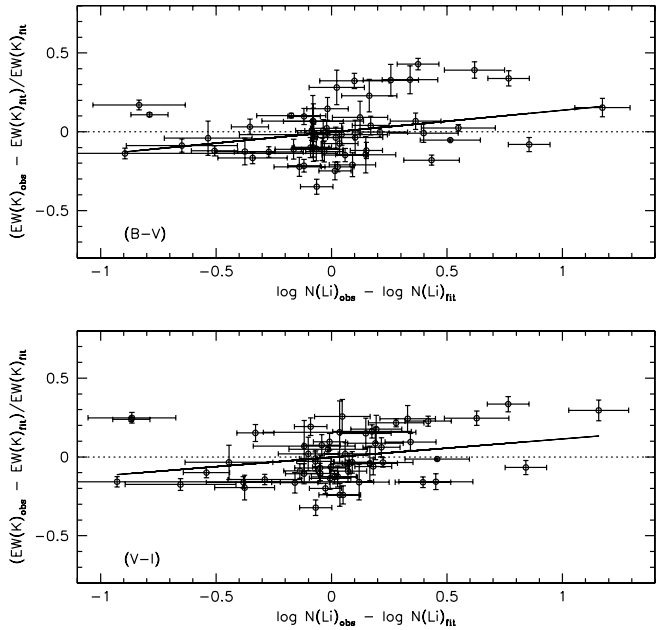

FIG. 9.—Differential λ7699 K I equivalent widths ([observed − fitted]/fitted) vs. our $(B-V)$-based (*top panel*) and $(V-I)$-based differential Li abundances (*bottom panel*).

First, there is the similarity in electronic configuration with the Li I atom and the fact that this particular K transition and the λ6707 Li I are both neutral resonance features. Second, the interplay of abundance and ionization effects leads to the happy circumstance that the line strengths of these two features are comparable in Pleiades dwarfs. Thus, line formation for both features should be similar in many respects.

The K I line strengths were taken from S93a and Jones et al. (1996b). These were then plotted versus $T_{\rm eff}$ as derived from both $B-V$ and $V-I$. The relation was well fitted by a fourth-order Legendre polynomial approximated by the relation $\mathrm{EW(K)} = 9098.151 - (4.126458 \times T) + (6.381173 \times 10^{-4} \times T^2) - (3.308942 \times 10^{-8} \times T^3)$ for the $B-V$ colors and by the relation $\mathrm{EW(K)} = 8926.171 - (4.170605 \times T) + (6.702972 \times 10^{-4} \times T^2) - (3.642286 \times 10^{-8} \times T^3)$ for the $V-I$ colors. These fits showed considerable scatter—the line-strength dispersion was $\sim$55 mÅ, which is considerably larger (and statistically significant) than even the maximum equivalent width errors estimated by S93a. So scatter is present in the potassium data as well.

Differential K I equivalent widths ([observed − fitted]/fitted) are plotted against the differential Li abundances in Figure 9. A correlation between the values is present, though with considerable scatter. The one-sided correlation coefficients are significant at the 99.0% and 98.3% confidence levels for the $(B-V)$ and $(V-I)$-based results. Such a correlation (of whatever magnitude), however, may arise not from some physical mechanism; instead, it may simply reflect correlated measurement errors.

Like the differential Li abundances, the differential K I line strengths are correlated with activity measure. Figure 10 shows the differential K I equivalent width versus the Ca II fluxes (*top panel*) and residual fluxes (*bottom panel*). The correlations are analogous to those seen for the differential Li abundances in Figure 8, and are significant at the $\sim$98.5% (top panel) and $\geq$99.9% (*bottom panel*) confidence levels.

4.2.2. *Calcium*

To examine the possibility of correlated measurement errors, we considered the line strengths of the λ6717 Ca I feature taken from S93a. These were fitted against $T_{\rm eff}$ in the same manner as the K I equivalent widths. The relations are given by $\mathrm{EW(Ca)} = 4203.706 - (1.859218 \times T) + (2.888087 \times 10^{-4} \times T^2) - (1.538325 \times 10^{-8} \times T^3)$ for the $B-V$ colors and by $\mathrm{EW(Ca)} = 2978.740 - (1.249348 \times T) + (1.887209 \times 10^{-4} \times T^2) - (9.973237 \times 10^{-9} \times T^3)$ for the $V-I$ colors. The scatter associated with these fits is

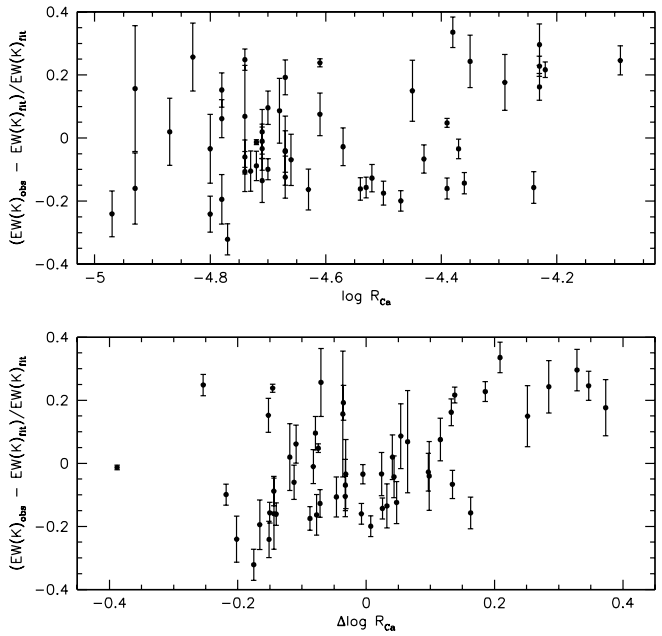

FIG. 10.—$(V-I)$-based differential K I line strengths are plotted vs. the Ca II infrared triplet flux ratio (*top panel*) and residual flux ratio (*bottom panel*).

$\sim$20 mÅ, which is consistent with the S93a uncertainties. Interestingly, unlike Li and K, there is no evidence for scatter in the calcium data above the measurement uncertainties. Differential Ca I equivalent widths are plotted against the differential Li abundances in Figure 11. The relation is flat. Unlike K, there is no significant correlation—the ordinary correlation coefficients are significant at only the $\sim$80% confidence level.

This indicates to us that the correlated scatter in Li and K line strengths is not due to measurement errors. Rather, we suggest that some physical mechanism affecting the details of line formation not included in standard LTE model photosphere analyses is the cause. Such a mechanism, if having star-to-star differences, may be the dominant source of the Li abundance scatter in Pleiades dwarfs. Since activity evinces such differences, it may naturally provide such a mechanism.

In an important theoretical study, Stuik et al. (1997) have urged similar caution in regarding Pleiades Li scatter as solely due to genuine abundance differences. These authors consider the photospheric effects of activity on Pleiades Li I and K I line strengths by modeling surface spots and plages. They can neither exclude nor confirm these particular manifestations of magnetic activity as the cause of the problematic and important K I variations in cool Pleiads. Their extensive efforts, though, do open the door for future improvement.

First, it seems important to establish whether their empirical solar-based spot/plage models or their "best-effort" theoretical stellar models are more nearly correct, and if one or the other model set is indeed applicable to all Pleiads since the two model sets produce color and line strength changes opposite in sign. Second, Stuik et al. (1997) note that their radiative equilibrium and mixed activity calculations depart from observations with increasing $(B-V)$. As they acknowledge, such disparities may signal other effects not yet considered: UV "line haze," which may depend on the presence and structure of an overlying chromosphere, impacting the details of line formation; unknown properties and effects of Pleiads' granulation patterns; and the influence of so-called solar-like "abnormal granulation" within plages. Third, other sources of nonthermal heating of the photosphere by chromospheric "activity" may need to be considered. Finally, simply relating colors or effective temperatures (from color-Teff conversions) of Pleiads having different activity levels may be more problematic than realized.

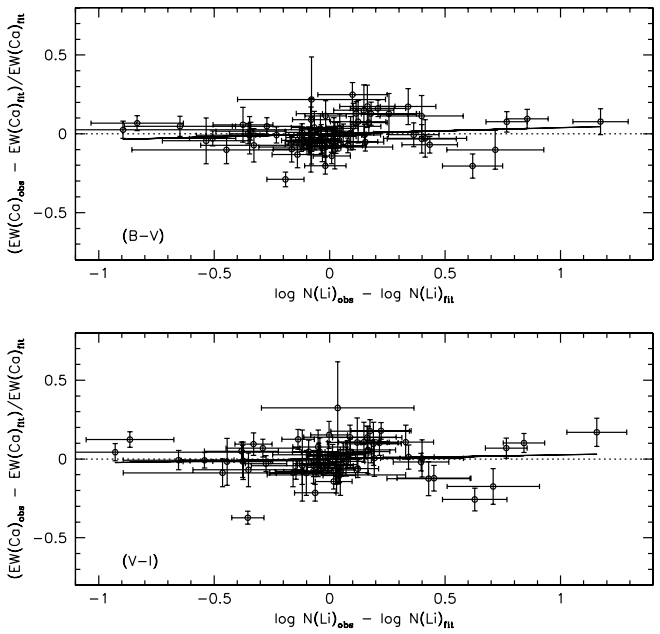

FIG. 11.—Differential λ6717 Ca I equivalent widths vs. our $(B-V)$-based (*top panel*) and $(V-I)$-based (*bottom panel*) differential Li abundances.

Houdebine & Doyle (1995) demonstrate that formation of the λ6707 Li I line is sensitive to activity in M dwarfs. The extent of these effects depends on the relative coverage of plages and spots. Houdebine & Doyle note the particular importance of the role of ionization in reducing the resonance line's optical depth. In late G and K dwarfs like those showing scatter in the Pleiades, star-to-star variations in departures of both photoionization and collisional ionization from that predicted by model photospheres might introduce significant star-to-star variations in the derived Li abundance.[6] Interestingly, King et al. (1999) find element-to-element abundance differences in two cool ($T_{\rm eff} \sim 4500$ K) Pleiades dwarfs and a similarly cool NGC 2264 PMS member that are ionization potential–dependent. We suggest that current evidence implicates nonphotospheric ionization differences as a likely source of star-to-star Li variations in the Pleiades.

5. OTHER MECHANISMS AND CONCERNS

5.1. *Metal Abundance Variations*

Variations in abundances of other elements can affect stellar Li depletion via the effects of stellar structure on PMS Li burning. For example, Figure 3 of Chaboyer et al. (1995), indicates that very small metal abundance differences of, say, 0.03 dex lead to substantial ($\gtrsim$0.3–0.4 dex) differences in PMS Li burning for $T_{\rm eff} \lesssim 4500$ K.

Extant studies (Boesgaard & Friel 1990; Cayrel, Cayrel, & Campbell 1988) of Pleiades F- and G-star iron abundances (which cannot simply be equated with "metallicity" when it comes to PMS Li depletion; Swenson et al. 1994) suggest no intrinsic scatter larger than 0.06–0.10 dex. The photometric scatter of the single stars in the color-magnitude diagram might allow a metallicity (or, perhaps more properly, those elements that are dominant electron donors in the stellar photospheres) spread of 0.05 dex. While small, these constraints would still permit substantial Li abundance spreads for *cool* Pleiads. Additionally, abundances of elements that may have a large impact on PMS Li depletion but little effect on atmospheric opacity (e.g., oxygen) have yet to be determined in cool Pleiades dwarfs.

However, the Li spread in the Pleiades extends to $T_{\rm eff}$ values substantially hotter than $\sim$4500 K. At hotter $T_{\rm eff}$ values, model PMS Li-burning is less sensitive to metallicity. For example, in the range 5000–5200 K, the observed Li abundance spread would require "metallicity" differences approaching a factor of 2. Such spreads would be surprising indeed, and not expected based on the limited results of extant Fe analyses of hotter cluster dwarfs. Abun-

[6] Overionization from photospheric convective inhomogeneities has been discussed in the context of Population II star Li abundances by Kurucz (1995).

dance differences (of a large number of elements) of this size would not be difficult to exclude with good quality spectra as part of future studies.

5.2. *Magnetic Fields*

Ventura et al. (1998) have recently investigated the effects of magnetic fields in stellar models and PMS Li depletion. They find that even small fields are able to inhibit convection, and thus PMS Li depletion. They suggest that a dynamo generated magnetic field linked to rotational velocity (thus, presumably yielding an association between activity and rotation given conventional wisdom) would result in zero-age main-sequence (ZAMS) star-to-star Li variations that mirror differences in star-to-star rotational (and presumably activity) differences. As these authors admit, the fits of their magnetic models to the Li-$T_{\rm eff}$ morphology and significant scatter of the Pleiades observations are not "perfect" or "definitive;" however, the qualitative agreement and ability to produce star-to-star scatter and general relations between Li abundance and rotation and activity are encouraging. Continued observations (especially detailed spectroscopic abundance determinations of various elements in numerous Pleiads) and theoretical work will be needed to establish the degree to which the Pleiades Li spread is illusory or real and, if the latter, its cause(s).

6. SUMMARY AND CONCLUSIONS

The very large dispersion in Li abundances at fixed $T_{\rm eff}$ in cool ($T \lesssim 5400$ K) Pleiads is a fundamental challenge for stellar evolution because standard stellar models of uniform age and abundance are unable to reproduce it. A variety of mechanisms (rotation, activity, magnetic fields, and incomplete knowledge of line formation) have been proposed to account for this scatter. Here, we construct a sample of likely single Pleiads and consider this problem with (1) differential Li abundances relative to a mean $T_{\rm eff}$ trend (2) rotational periods instead of projected rotational velocities (3) chromospheric emission indicators, and (4) line strengths of other elements.

We calculated $T_{\rm eff}$ values from both $(B-V)$ and $(V-I)$ on a self-consistent scale based on the calibrations of Bessell (1979). We find differences in the two $T_{\rm eff}$ values and these are significantly correlated with both general activity level and with differences in activity, suggesting that surface inhomogeneities may noticeably affect stellar colors. Our results are consistent with a growing body of evidence of significant differences between $(B-V)$- and $(V-I)$-based $T_{\rm eff}$ values, a propensity for $(B-V)$ to yield larger $T_{\rm eff}$ values, and a relation of these characteristics with activity in young stars from 5 Myr old PMS stars in NGC 2264 (Soderblom et al. 1999) to PMS stars in the 30 Myr old IC 2602 (Randich et al. 1997) to ZAMS stars in the $\sim$100 Myr old Pleiades.

However, the similarity between the sensitivity of the derived Li abundance to $T_{\rm eff}$ and the clusters' physical Li-$T_{\rm eff}$ morphology means that even substantial $T_{\rm eff}$ errors are not a significant source of star-to-star Li scatter. Nor are observational errors. Comparison of the scatter in the differential Li abundances with errors from $T_{\rm eff}$ and line-strength uncertainties indicates an infinitesimal probability that the observed scatter occurs by chance. We find significant scatter in the Li abundances below $\sim$6000 K; it is significantly larger, though, below $\sim$5500 K. Statistical analysis fails to support previous claims of smaller scatter in the late K dwarfs relative to the late G and early-mid K dwarfs.

There is a spread of Li abundance at low $v \sin i$, whereas the rapid projected rotators tend to have larger differential Li abundances in the range $4500 \leq T_{\rm eff} \leq 5500$. However, use of photometric rotation periods (free from uncertainties in the inclination angle i) indicates there is *not* a one-to-one mapping between differential Li abundance and rotation. The stars H II 263, 320, and 1124 are examples of stars with Li excesses but slow rotation ($P = 4.6$–6.1 days). In contrast to previous claims based on $v \sin i$, the rotation periods indicate a true range of Li abundance with rotation in the mass bin 0.7–0.9 $M_{\odot}$.

Using the theoretical framework of Krishnamurthi et al. (1997), we constructed stellar models to investigate the hydrostatic effects of rotation on stellar structure and PMS Li burning. As shown in Figure 8, these models fail to account for the Pleiades Li dispersion, which is in agreement with the independent conclusions of Mendes et al. (1999).

We find that the star-to-star differences in Pleiades Li abundances are correlated with activity differences, as measured from Ca II infrared triplet flux ratios, at a statistically significant level. Moreover, the Li differences are significantly correlated with differences in the strengths of the λ7699 K I resonance feature. This seems to not be due to correlated measurement errors since the Li differences show no correlation with the λ6717 Ca I line-strength residuals. This is a significant result given similarities in the Li and K feature's atomic properties and line strengths. We suggest that incomplete treatment of line formation, related to activity differences, plays a significant role in the Li dispersion—i.e., that part of the dispersion is illusory. As emphasized by Houdebine & Doyle (1995), the formation of the Li I feature is sensitive to ionization conditions. If chromospheric activity variations can produce significant variations in photo- and collisional-ionization in the Li I line formation region not accounted for by LTE analyses using model photospheres, this may lead to errors in the inferred abundance. Relatedly, we note the results of King et al. (2000) who found ionization potential-dependent effects in the elemental abundances of two cool ($T_{\rm eff}$) Pleiads and a similarly cool NGC 2264 PMS star.

If such conjecture is correct, we expect that somewhat older (less active) cluster stars will exhibit less Li dispersion. This seems to be the case for the $\sim$800 Myr old Hyades cluster (Thorburn et al. 1993) and perhaps also for the mid-G to mid-K stars in M34 (Jones et al. 1997). These clusters still exhibit scatter, and this may be real and due to differences in depletion from structural effects of rotation (Mendes et al. 1999), magnetic fields (Ventura et al. 1998), small metallicity variations (§ 5.1), main-sequence depletion due to angular momentum transport from spin-down (Pinsonneault et al. 1990; Charbonnel, Vauclair, & Zahn 1992) or a planetary companion (Cochran et al. 1997), and photospheric accretion of circumstellar/planetary material (Alexander 1967; Gonzalez 1998). The amount of scatter expected in even older clusters is less clear. If, e.g., rotationally induced mixing acts over longer timescales then the scatter may well increase again; indeed, the substantial Li scatter in M67 solar-type stars observed by Jones, Fischer, & Soderblom (1999) could indicate that this is the case.

These authors called attention to the possible pattern of very large Li scatter in young clusters, considerably reduced

scatter in intermediate-age clusters, and increased scatter in older clusters. In the scenario we envision, variations in activity-regulated ionization of the Li I atom may be responsible for the majority of (mostly illusory) star-to-star Li differences in near-ZAMS and younger stars; of course, this does not exclude a (lesser) role from other variable mechanisms influencing PMS Li burning. If the decline in the activity level of intermediate-age stars reduces the importance of variable ionization, then the (smaller) Li scatter in these stars could arise from variations in PMS Li burning due to, e.g., the hydrostatic effects of rotation on stellar structure, inhibition of convection by magnetic fields, and small metallicity variations; additional contributions may come from processes just beginning to become effective for ZAMS stars such as rotationally induced mixing and planetary/circumstellar accretion. In older stars such as M67, the increase in scatter (and overall Li depletion) is then a product of processes efficiently acting on the main-sequence proper such as rotationally induced mixing and/or photospheric accretion.

Distinguishing specific mechanisms and their relative importance for Li depletion and scatter at a given age will require continuing observational and theoretical efforts. Important advances on the theoretical front are at least threefold: continued investigation of the role of magnetic fields in PMS Li depletion, realistic model atmospheres that include chromospheres, and detailed non-LTE abundance calculations which employ these to extend sophisticated modeling attempts (e.g., Stuik et al. 1997). On the observational front, continued observations of Li in a variety of clusters spanning a range in age and metallicity are needed. We believe that particularly important observational work to be accomplished includes the determination of photometric periods in more cluster stars, detailed abundances of numerous elements (in particular, using both ionization sensitive and ionization insensitive features and elements) in cluster stars, quantification of even small "metal" (not just Fe) abundance spreads in cluster stars, and the association between planetary systems and parent star Li and light metal abundances.

REFERENCES

Alexander, J. B. 1967, Observatory, 87, 238
Anders, E., & Grevesse, N. 1989, Geochim. Cosmochim. Acta, 53, 197
Bahcall, J. N., & Ulrich, R. K. 1988, Rev. Mod. Phys., 60, 297
Balachandran, S., Lambert, D. L., & Stauffer, J. R. 1988, ApJ, 333, 267
———. 1996, ApJ, 470, 1243
Bessell, M. S. 1979, PASP, 91, 589
Bodenheimer, P. 1965, ApJ, 142, 451
Boesgaard, A. M., Budge, K. G., & Ramsay, M. E. 1988, ApJ, 327, 389
Boesgaard, A. M., & Friel, E. D. 1990, ApJ, 351, 467
Bouvier, J., Rigaut, F., & Nadeau, D. 1997, A&A, 323, 139
Butler, R. P., Cohen, R. D., Duncan, D. K., & Marcy, G. W. 1987, ApJ, 319, L19
Cayrel, R., Cayrel de Strobel, G., & Campbell, B. 1988, in The Impact of Very High S/N Spectroscopy on Stellar Physics, ed. G. Cayrel de Strobel and M. Spite, (Dordrecht: Kluwer), 449
Chaboyer, B., Demarque, P., & Pinsonneault, M. H. 1995, ApJ, 441, 876
Charbonnel, C., Vauclair, S., & Zahn, J.-P. 1992, A&A, 255, 191
Cochran, W. D., Hatzes, A. P., Butler, R. P., & Marcy, G. W. 1997, ApJ, 483, 457
Endal A. S., & Sofia, S. 1979, ApJ, 232, 531
Garciá Lopez, R. J., Rebolo, R., Magazzu, A., & Beckmann, J. E. 1991a, Mem. Soc. Astron. Italiana, 62, 187
Garciá Lopez, R. J., Rebolo, R., Beckmann, J. E., & Magazzu, A. 1991b, in The Sun and Cool Stars: Activity, Magnetism, Dynamos, ed. I. Tuominen, D. Moss, & G. Rüdiger (Berlin: Springer), 443
Garciá Lopez, R. J., Rebolo, R., & Martiń, E. L. 1994, A&A, 282, 518
Gonzalez, G. 1998, A&A, 334, 221
Houdebine, E. R., & Doyle, J. G. 1995, A&A, 302, 861
Jones, B. F., Fischer, D., & Soderblom, D. R. 1999, AJ, 117, 330
Jones, B. F., Fischer, D. A., & Stauffer, J. R. 1996a, AJ, 112, 1562
Jones, B. F., Shetrone, M., Fischer, D., & Soderblom, D. R. 1996b, AJ, 112, 186 (JSFS)
Jones, B. F., Fischer, D., Shetrone, M., & Soderblom, D. R. 1997, AJ, 114, 362
King, J. R. 1998, AJ, 116, 254
King, J. R., Soderblom, D. R., Fischer, D., & Jones, B. F. 2000, ApJ, in press
Krishnamurthi, A., Pinsonneault, M. H., Barnes, S., & Sofia, S. 1997, ApJ, 480, 303
Krishnamurthi, A., et al. 1998, ApJ, 493, 914
Kurucz, R. L. 1995, ApJ, 452, 102
Magazzu, A., Rebolo, R., & Pavelenko, I. V. 1992, ApJ, 392, 159
Magnitskii, A. K. 1987, Soviet Astron. Lett., 13, 457
Martin, E. L., & Claret, A. 1996, A&A, 306, 408
Mendes, L. T. S., D'Antona, F., & Mazzitelli, I. 1999, A&A, 341, 174
Mermilliod, J.-C., Rosvick, J. M., Duquennoy, A., & Mayor, M. 1992, A&A, 265, 513
Pilachowski, C. A., Booth, J., & Hobbs, L. M. 1987, PASP, 99, 1288
Pinsonneault, M. 1997, ARA&A, 35, 557
Pinsonneault, M. H., Kawaler, S., & Demarque, P. 1990, ApJS, 74, 501
Pinsonneault, M. H., Stauffer, J., Soderblom, D. R., King, J. R., & Hanson, R. B. 1998, ApJ, 504, 170
Prosser, C. F., et al. 1993, PASP, 105, 407
———. 1995, PASP, 107, 211
Randich, S., Aharpour, N., Pallavicini, R., Prosser, C. F., & Stauffer, J. R. 1997, A&A, 323, 86
Russell, S. C. 1996, ApJ, 463, 593
Skrutskie, M. F., Dutkevitch, D., Strom, S. E., Edwards, S., Strom, K. M., & Shure, M. A. 1990, AJ, 99, 1187
Soderblom, D. R., Jones, B. F., Balachandran, S., Stauffer, J. R., Duncan, D. K., Fedele, S. B., & Hudon, J. D. 1993a, AJ, 106, 1059 (S93a)
Soderblom, D. R., King, J. R., Siess, L., Jones, B. F., & Fischer, D. 1999, AJ, 118, 130
Soderblom, D. R., Stauffer, J. R., Hudon, J. D., & Jones, B. F. 1993b, ApJS, 85, 315
Stauffer, J. R., & Hartmann, L. W. 1987, ApJ, 318, 337
Stauffer, J. R., Schild, R. A., Baliunas, S. L., Africano, J. L. 1987, PASP, 99, 471
Stuik, R., Bruls, J. H. M. J., & Rutten, R. J. 1997, A&A, 322, 911
Swenson, F. J., Faulkner, J., Iglesias, C. A., Rogers, F. J., & Alexander, D. R. 1994, ApJ, 422, L79
Tassoul, J.-L. 1978, in Theory of Rotating Stars (Princeton: Princeton Univ. Press), 188
Thorburn, J. A., Hobbs, L. M., Deliyannis, C. P., & Pinsonneault, M. H. 1993, ApJ, 415, 150
Van Leeuwen, F., Alphenaar, P., & Meys, J. J. M. 1987, A&AS, 67, 483
Ventura, P., Zeppieri, A., Mazzitelli, I., & D'Antona, F. 1998, A&A, 331, 1011
Zahn, J.-P. 1983, in Astrophysical Processes in Upper Main-Sequence Stars, ed. B. Hauck & A. Maeder (Geneva: Geneva Obs.), 253
———. 1992, A&A, 265, 115